

Electro-optical and dielectric properties of CdSe quantum dots and 6CHBT liquid crystals composites

U. B. Singh,¹ R Dhar,² A. S. Pandey,² S. Kumar,³ R. Dabrowski,⁴
and M. B. Pandey^{1,a}

¹Department of Physics, Vikramajit Singh Sanatan Dharama College, Kanpur-208002, India

²Centre of Material Sciences, Institute of Interdisciplinary Studies, University of Allahabad, Allahabad-211002, India

³Raman Research Institute, C. V. Raman Avenue, Bangalore-560080, India

⁴Institute of Applied Sciences and Chemistry, Military University of Technology, 00-908-Warswa, Poland

(Received 19 July 2014; accepted 4 November 2014; published online 11 November 2014)

We have prepared the composites of a room temperature nematic liquid crystal namely 4-(trans-4-n-hexylcyclohexyl) isothiocyanatobenzoate (6CHBT) and Cadmium Selenide Quantum Dots (CdSe-QDs) and investigated their electro-optical and dielectric properties. Effect of dispersion of CdSe-QDs on various electro-optical and display parameters of host liquid crystalline material have been studied. Physical parameters, such as switching threshold voltage and splay elastic constant have been altered drastically for composites. Dispersion of QDs in a liquid crystals medium destabilizes nematic ordering of the host and decreases the nematic-to-isotropic transition temperature. © 2014 Author(s). All article content, except where otherwise noted, is licensed under a Creative Commons Attribution 3.0 Unported License. [<http://dx.doi.org/10.1063/1.4901908>]

I. INTRODUCTION

The dispersion and self-assemblies of nanostructures in liquid crystal (LC) media has emerged as an exciting field of research in recent years because of their potential for application and ease to control the orientation of host and self-assembled structure by external stimulus.¹ The combination of geometrical order, optical & electrical response and soft elasticity of liquid crystals make them also suitable to study the topological defects created by nanostructure/micro-particles in LC medium.¹⁻³ Further this area of research has enormous potential for fundamental studies due to enhanced organizational complexity of the composites.^{2,3} LC are organic, shape-anisotropic compounds that give rise to mesophases characterized by long-range orientational and/or one-dimensional translational order while overall maintaining fluid characteristics, such as high mobility at the molecular level and fast responses to external fields and mechanical stresses.⁴ Hence LC materials have been used as a smart fluid for dispersion of nano structures (for example- nanoparticles, nanotubes, and quantum-dots) and micro-particles since last decade because of its elastic mediated interaction between medium and alien objects which is promising for directed assembly of nanostructures.^{5,6} The assembly of nanostructures and LC could be re-oriented by external inducement for example: by applying electric and magnetic field.⁷ The small inclusion of carbon nanotubes (CNTs),^{8,9} nano-particles (NPs),¹⁰⁻¹³ nano-wires¹⁴ and graphene¹⁵ in LC medium has been reported and the effects of inclusion of nanostructures on physical properties of host have been demonstrated. It is found that the incorporation of NPs/CNTs enhances the electro-optical properties of the liquid crystals itself with ease of alignment of composites.¹¹⁻²³ The inorganic nano-particles known as quantum dots (QDs) have semiconducting properties and have zero dimension due to their tiny sizes.²⁴ They have been the focal point of research in vast areas such as medicine, photonics, and optoelectronic devices due to their promising application.²⁵ Assembling

^a Author for correspondence. E-mail: mbpandey@gmail.com



of QDs into nanoscale configurations over macroscopic dimensions is an important goal to realize their potential applications. It should be noted that the use of QDs in optoelectronics requires their incorporation into a matrix.²⁶ There are few studies on dispersion of QDs in LC medium and exploration of physical properties of composites. In principle, anisotropic properties of LC can facilitate assembly of QDs in nearly one-dimensional chain-like structures along the nematic director and these assemblies of QDs can be controlled by external electric fields. On the other hand unique optical and electronic properties of QDs might be useful to enhance electro-optical properties of LC host. In the present article, we are reporting electro-optical and dielectric properties of the composites prepared by dispersion of CdSe-QDs in a room temperature nematic liquid crystal 4-(trans-4-n-hexylcyclohexyl) isothiocyanatobenzoate (6CHBT).

II. EXPERIMENTAL TECHNIQUES

A. Synthesis of quantum dots (QDs)

In a typical synthesis, trioctyl phosphine-selenium (TOP-Se) stock solution was prepared by adding 0.3974 g of selenium powder to 3.7 g of TOP in a round bottom flask and the mixture was heated to 150°C under argon flow to obtain a clear solution. In another flask, 0.225 g of cadmium oxide (CdO) and 4 g of stearic acid were heated to 150°C under argon flow. Once CdO was dissolved, the solution was cooled to room temperature. 8 g of trioctyl phosphine oxide (TOPO), 3.18 g of octadecyl amine were subsequently added and heated to 150°C. At this temperature, 2ml of TOP-Se stock solution was swiftly injected into the Cd solution to induce the growth of quantum dots. Two different sizes of quantum dots were obtained by maintaining the temperature of reaction mixture at 120°C and 130°C for 30 min respectively in two different batches. The reaction mixture was added to toluene, to terminate further reaction. Methanol was subsequently added to the toluene dispersion for crashing out QDs. The excess reaction precursors and capping agents were removed by repeated washing with methanol and dispersing in toluene, the purified QDs were collected after centrifugation. The details of synthesis of QDs are reported elsewhere.²⁷ The sizes of QDs have been determined by UV Spectrometer made by Simazdu. Chloroform was used as a reference and small amount of CdSe-QDs have been added to it. The reference & composite samples have been put in the Cabinet and UV absorption spectra have been recorded.

B. Composite preparation and characterization techniques

A small weight percents (0.01 & 0.02 wt %) of CdSe-QDs have been added in a liquid crystalline material 6CHBT. The composites have been sonicated in the isotropic phase of LC for homogeneous dispersions. The thermodynamical studies of the pure and composites samples have been carried out with the help of Differential Scanning Calorimeter (DSC) of NETZSCH model DSC-200-F3-Maia. Peak transition temperatures (T_p) have been determined with the accuracy of 0.1 °C for fully-grown peaks. The cells were made from indium tin oxide (ITO) coated glass electrodes in the form of parallel plate capacitor and the thickness of the used cells were $7.2 \pm 0.2 \mu\text{m}$. The inner surfaces of cells have been coated with nylon polymer and parallel-rubbed for planar alignment with a pre-tilt angle of $\sim 5^\circ$ (made by Instec, USA). For electro-optical measurements, the pure LCs and composites have been filled in the cells by capillary action. Homogeneous dispersion of QDs in LCs matrix and their alignment was examined under a Polarized Optical Microscope (POM). The transmission intensity of white light, passing through cells, was measured using a photo-detector (made by Instec, USA) mounting on POM. These cells have also been used to measure the transverse component of relative permittivity (ϵ'_\perp). To measure the longitudinal component of relative permittivity (ϵ'_\parallel), inner surfaces of ITO coated glass plates were treated with lecithin which promote normal anchoring of LC molecules. In this case, the thickness of used cell was $\sim 10 \mu\text{m}$, which was fixed by using Mylar spacers. Dielectric data have been acquired by using a Newton's Phase Sensitive Multimeter (model PSM1735) coupled with an Impedance Analysis Interface (IAI model-1257) in the frequency range of 1 Hz–35 MHz. The relative permittivity (ϵ'), dielectric loss (ϵ'') and other parameters have been obtained from the measured capacitance

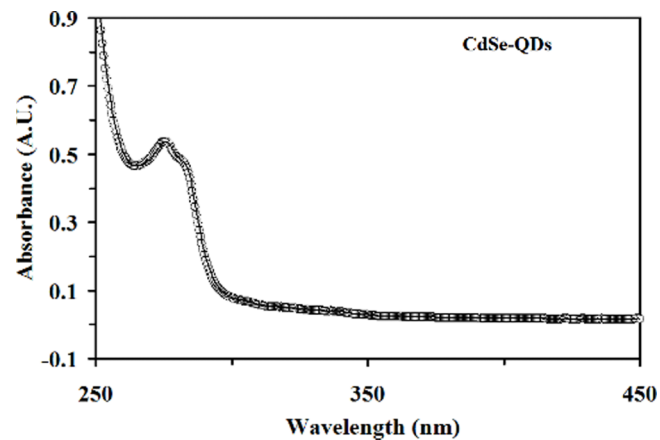


FIG. 1. Optical absorption spectra of Cadmium Selenide Quantum Dots (CdSe-QDs) taken by UV-Visible absorption Spectrometer.

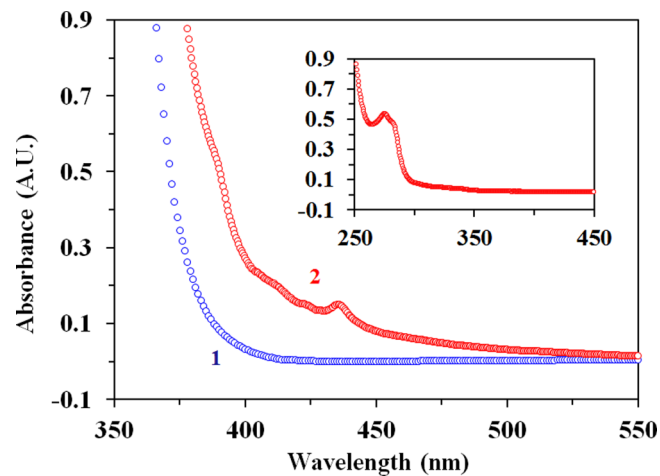


FIG. 2. Optical absorption spectra of 0.01% CdSe-QDs dispersed in 6CHBT showing the Red shift of absorption peak corresponding to pure CdSe-QDs which is shown in the inset.

and conductance data of the cell filled with samples as described earlier.¹² The temperature of the samples for dielectric and electro-optical studies have been controlled with the help of a hot stage from Instec (model HS-1) having an accuracy of ± 0.1 °C and a temperature resolution of 3 mK.

III. RESULTS AND DISCUSSION

A. Characterization of QDs in composites

The sizes of QDs have been calculated from recorded UV absorption spectra. In Fig. 1, an absorption peak has been observed at 270 nm. The sizes of QDs have been found to be ~ 3.5 nm. The sizes of QDS have been confirmed by SEM as well.²⁷ Optical absorption spectra of CdSe-QDs dispersed in 6CHBT is given in Fig. 2. Absorption spectra of composites show the redshift due to dielectric divergence between QDs and surrounding host LCs medium. From an application point of view, this phenomenon might be utilized to develop Liquid Crystal Filters (LCFs). This type of filters might be useful to design electronic imaging devices, such as charge-coupled devices (CCDs), because it could offer excellent imaging quality with a simple linear optical pathway in the visible wavelength region (400 to 700 nm).

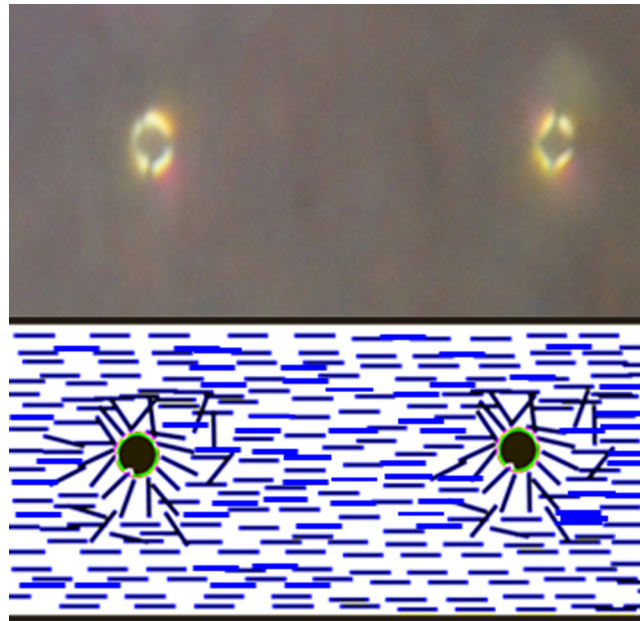


FIG. 3. (a) Polarizing Optical Microscope (POM) textures showing LC alignment around QDs clusters and far-field director (b) a sketch diagram showing far field LC director and local orientation of LC molecules around QDs clusters.

B. Transition temperature, optical and electro-optical studies of the composites

The dispersion of QDs in LCs matrix of the composites have been examined under POM ($\times 200$) and the optical textures have been recorded with the help of a digital camera. As most parts of the samples have dark patches under crossed polarizer which suggest that QDs are well dispersed in LCs and far field nematic director of LCs follow planar alignment due to confined glass plates. However, some big particles due to coagulation of QDs are also seen under POM. They are termed QDs clusters hereafter. Around some of the QDs clusters, a well patterned bright defect structures with four extinction lines have been observed due to normal (homeotropic) anchoring of LC molecules on their surfaces (see Fig. 3). These defects have a signature similar to structures formed around homeotropic micro-particles immersed in LCs.^{2,3,5,6} Under POM observation, it is found that the turbidity of composite clears at lower temperature in comparison to pure LCs. This happens because of nematic to isotropic transition (T_{NI}) of composites has been reduced considerably in presence of QDs. A typical DSC plot, for pure LCs and 0.01% CdSe-QDs composite, has been shown in Fig. 4 which also confirms the POM observation.

The intensity of transmitted light with applied ac voltage has been measured in terms of photo-voltage which is used to plot the Transmission-Voltage (T-V) characteristics. Switching threshold voltages (V_{th}) have been determined from the T-V curves. T-V curves for pure and composites are shown in Fig. 5. When applied voltage was low, LC molecules lie in the plane of the cell due to planar anchoring at bounding glass surfaces. Consequently bright state is observed under POM which is maximum intensity in T-V curves. This state continues from low voltages up to 0.76 V for pure 6CHBT, 0.41 V for 0.01% QDs- 6CHBT and 0.34 V for 0.02% QDs-6CHBT composites. When applied voltage has been increased from aforementioned values, corresponding to respective samples, intensity of transmitted light diminishes gradually and ultimately minimum intensity of light has been observed which corresponds to the dark state for respective samples. This happens due to the reorientation of LC molecules perpendicular to bounding glass electrodes i.e. LC molecules have been realigned along the direction of applied electric field. This phenomenon is called Frederick transition which is independent of sample thickness and the corresponding voltage is called switching threshold voltage (V_{th}). The voltage required to reduce the intensity of transmitted light across cell from 90 to 10 % of the maximum values is called switching voltage interval. It is observed that V_{th} decreases drastically $\sim 46\%$ & $\sim 55\%$ for 0.01 and 0.02 wt% QDs-6CHBT

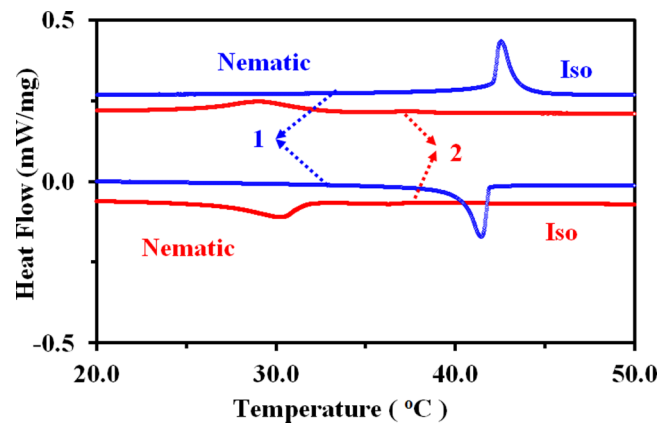


FIG. 4. DSC thermograms of the pure (blue curve) and 0.01 wt % CdSe-QDs dispersed 6CHBT (red curve) showing nematic to isotropic transitions in the heating and cooling cycles at the scan rate of 5 °C/min.

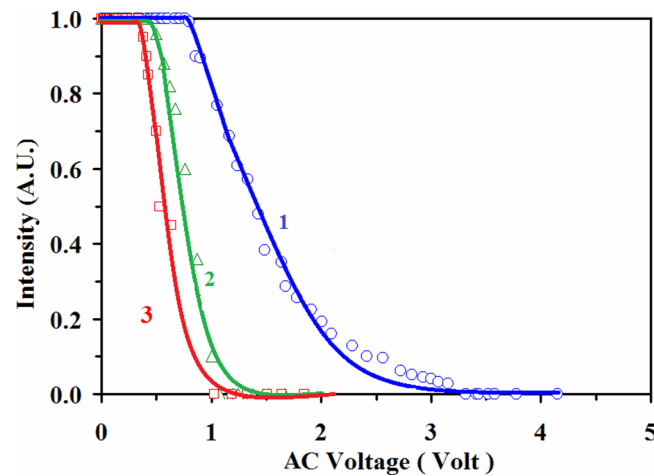


FIG. 5. Transmission-Voltage (T-V) characteristic of the cells filled with samples to the applied alternating voltage of frequency 1 kHz. Curves 1 (Blue), 2 (Green) and 3 (Red) are corresponding to the pure, 0.01 and 0.02 wt% CdSe-QDs dispersed in 6CHBT respectively.

composites respectively. Steepness of T-V curves has been calculated from Fig. 5 which is also a measure of switching voltage interval. Steepness of T-V curve has also been increased for composites with respect to pure samples.

The static values of relative permittivities (transverse ϵ_{\perp}' and longitudinal ϵ_{\parallel}') have been obtained from dielectric measurements and their temperature variation is shown in Fig. 6(a). Dielectric anisotropies ($\Delta\epsilon'$) of the composites increases on decreasing temperature and its saturates at ~ 20.0 °C (Fig. 6(b)). The values of $\Delta\epsilon'$ have been found to be approximately same for pure and composites samples at ~ 20.0 °C. Hence electro-optical experiments have been performed at this temperature and the values of $\Delta\epsilon'$ and V_{th} have been used to calculate the splay elastic constants (K_{11}) from the equation:

$$V_{th} = \pi \left(\frac{K_{11}}{\epsilon_0 \Delta\epsilon'} \right)^{\frac{1}{2}} \quad (1)$$

This equation suggests that square of V_{th} is directly proportional to K_{11} and inversely proportional to $\Delta\epsilon'$ of the material. Taking experimental values of V_{th} and $\Delta\epsilon'$ at 20 °C, K_{11} have been determined from this equation and listed in Table I. The presence of spherically symmetric CdSe-QDs in the liquid crystalline 6CHBT matrix is responsible for the decrease of K_{11} . Such results have also been found in our previous studies for silver nanoparticles dispersed LCs.¹²

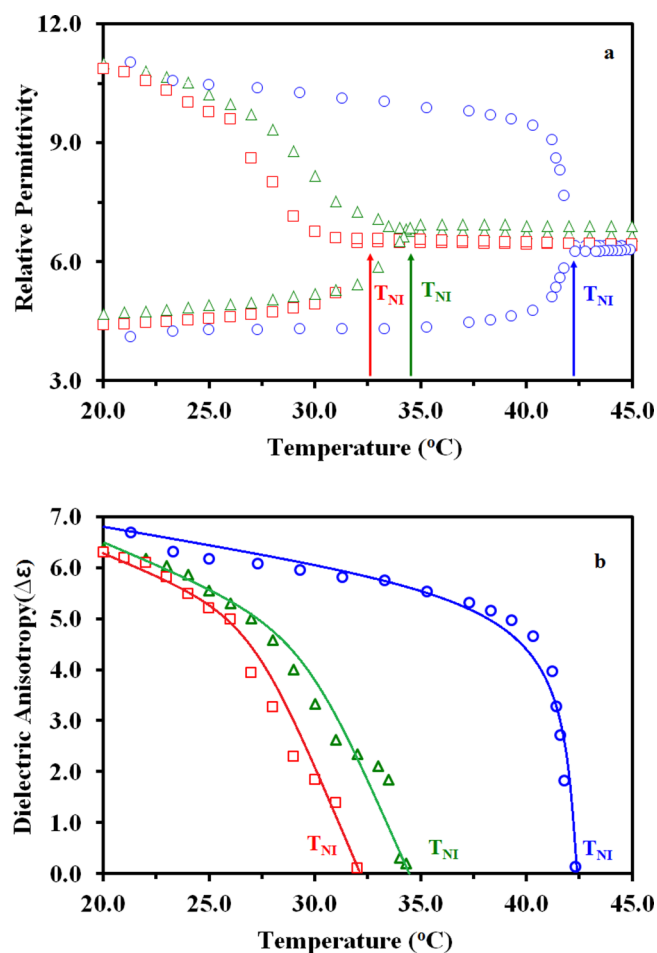


FIG. 6. (a) Variation of relative permittivities (transverse ϵ_{\perp}' and longitudinal ϵ_{\parallel}') and (b) dielectric anisotropies ($\Delta\epsilon'$) with temperature for pure and CdSe-QDs dispersed in 6CHBT. Circle, triangle and square respectively represent the data corresponding to the pure, 0.01 and 0.02 wt% CdSe-QDs dispersed in 6CHBT.

TABLE I. Transition temperature (T_{NI} in $^{\circ}\text{C}$), Threshold voltage (V_{th} in V), Dielectric anisotropy ($\Delta\epsilon'$), splay elastic constant (K_{11} in pN), and the ratio of the dielectric anisotropy to the transverse component of the dielectric permittivity ($\Delta\epsilon'/\epsilon_{\perp}'$) of pure 6CHBT and QDS dispersed samples.

Sample	T_{NI}	V_{th}	$\Delta\epsilon'$	K_{11}	$\Delta\epsilon'/\epsilon_{\perp}'$
6CHBT pure	42.0	0.76	6.9	3.17	1.68
6CHBT (0.01 wt% CdSe-QDs)	34.0	0.41	6.5	0.98	1.41
6CHBT (0.02 wt% CdSe-QDs)	32.5	0.34	6.4	0.66	1.45

C. Dielectric properties of composites:

In the isotropic phase (see Fig. 6(a)), there is no preferred orientation of the molecules and the distribution of their centre of mass are isotropic within cells. Hence measured relative permittivities in both cells (planar and homeotropic) have approximately equal values (ϵ_{iso}). On lowering the temperature below 42 $^{\circ}\text{C}$ for pure samples, measured permittivities in two cells are no longer equal which suggest that orientational ordering is taking place and medium is no longer isotropic. However, in the case of cells filled with composites, this phenomenon occurred at lower temperatures about $\sim 34.0^{\circ}\text{C}$ and $\sim 32.5^{\circ}\text{C}$ for 0.01% and 0.02% QDs dispersed samples respectively (Fig. 6(b)). This is in conformity to POM and DSC investigations, which suggest that T_{NI} reduced enormously for composites. It is also observed that the values of ϵ_{\perp}' and ϵ_{\parallel}' do not saturates quickly just below

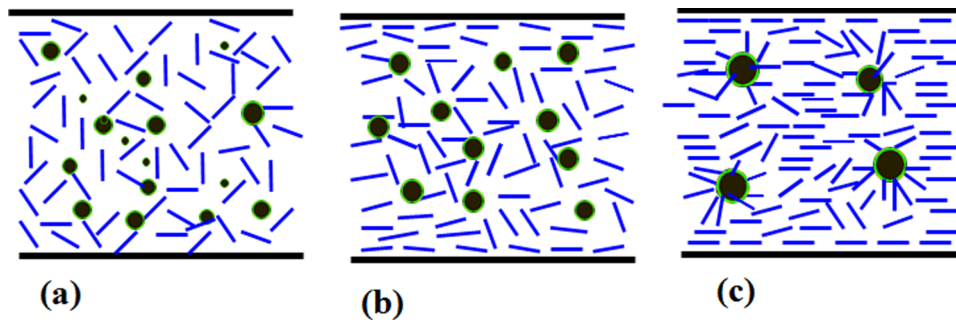


FIG. 7. A sketch diagram showing the orientation of LC molecules around QDs clusters (shown by blue nails) confined in the cell treated for planar alignment of LC; In the isotropic (a, b) and nematic phases (c) of the composites. QDs clusters have been shown by black dots.

T_{NI} for composites as was the case of pure samples. Their values changes gradually and becomes invariant and approximately equal to the values of pure samples at about $\sim 20^\circ\text{C}$. This suggests that there is a competition between QDs and LCs host to retain isotropic and nematic state respectively. This phenomenon could be explained by a sketch diagram as shown in Fig. 7. LCs molecules are randomly distributed in the cells and around QDs surfaces in the isotropic phase (Fig. 7(a)). The effect of CdSe-QDs on the phase transition of composites depends on the surface anchoring of the LC molecules around QDs and their clusters. On lowering the temperature (below T_{NI} of pure sample), LCs molecules in the cells try to arrange themselves along far field nematic director due to anchoring at the bounding glass plates. But local ordering effect of QDs surfaces is randomly arranged, this can lead to a random-field effect and an overall disordering of the composites and thus destabilizing the nematic phase (Fig. 7(b)). In this case, the QDs act either as foreign/nucleation sites for local ordering or as disordering sites for orientation along far field nematic director that stabilizes the isotropic phase and causes reduced T_{NI} for composites. On further lowering the temperature, there is a competition between bounding glass plates and QDs for local ordering. LC molecules in the vicinity of QDs surfaces align such a way that minimizes interfacial energy due to specific surface anchoring between QDs and LC molecules (Fig. 7(c)). It is clear from Fig. 3, LC molecules anchored strongly near the surface of QDs and formed a well pattern defects with four extinction lines. LC molecules forming these defects are disoriented from the far-field nematic director. It might also be possible that some of the tiny QDs clusters combined together to minimize total energy of the systems associated with splay, twist and bend due to local orientation of LCs around QDs cluster and hence stabilizing the nematic phase. Viscosity of host medium also increases upon lowering temperature and the alignment of the samples improve due to bounding glass plates. These combined effects forces nematic ordering to take place in the composites samples and phase transition occurred.

From dielectric spectrum, it has been observed that relative permittivity in planar configuration of nematic phase is almost constant with the frequency range from 100Hz to 1MHz, implying that no dipolar relaxation phenomenon occurs in this frequency range. However, for homeotropically aligned samples, a relaxation mode in the MHz frequency region is detected which corresponds to the flip-flop motion of the LC molecules about their short axes.²⁸ Relaxation frequencies corresponding to the flip-flop motion follow Arrhenius behavior. The relationship between frequency (f_R) and activation energy (W_A) corresponding to the flip-flop motion of molecules about their short axes is governed by equation:

$$f_R = A \exp(-W_A/N_A kT) \quad (2)$$

Where N_A is the Avogadro number, k is the Boltzmann constant. The logarithm of relaxation frequency versus inverses of the temperature plots is found to be linear (see Fig. 8). The activation energies were calculated from the slopes of the respective plots which have been obtained by the method of least square fit. The activation energies are found to be 37.4, 49.7 and 40.7 kJ/mol

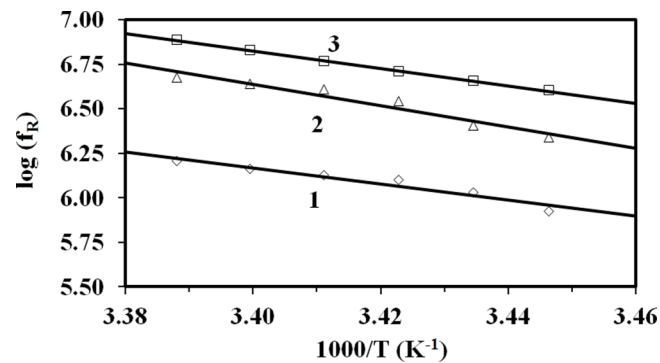


FIG. 8. Variation of logarithm of relaxation frequency with inverse of absolute temperature (K^{-1}) showing Arrhenius behavior. Curves 1 (diamond), 2 (triangle) and 3 (square) correspond to the pure, 0.01% and 0.02% CdSe-QDs dispersed in 6CHBT respectively.

respectively for pure LC, 0.01% and 0.02% QDs dispersed composite systems. The values of activation energy are increasing for composite with respect to pure samples, which support the local disordering effects of the QDs that destabilize the nematic phase.

IV. CONCLUSIONS

We have demonstrated the immense effects of QDs dispersion on electro-optical and dielectric properties of the host LC. The composites are shown to have enhance electro-optical properties. The threshold voltage required to switch the LC molecules from planar (bright state) to homeotropic (dark state) configuration is substantially reduced for composites due to dispersion of the QDs. The dispersion of QDs also reduces the nematic ordering of host medium which causes lowering of nematic to isotropic transition for composites. The observation of four extinction lines between crossed polarizers around the QD clusters reveals that nematic order around the QD clusters differs from the far-field nematic order. This is helpful to understand the mechanism of interaction between LCs and the QDs. This could be utilized to formulate fundamental theories of intermolecular interactions and self-organization. Due to dielectric divergence between QDs and surrounding host medium, the absorption spectrum of QDs shows Red Shift for studied composite systems. These properties of the composites make them suitable to design new devices based on QDs-LC.

ACKNOWLEDGMENTS

This work is financially supported by DAE (BRNS) Govt of India vide project no. 2010/20/37P/4/BRNS/1591. UBS thanks DAE (BRNS) for Research Fellowship under the project. MBP acknowledges the support of DST, Government of India through Young Scientist Project award (SR/FTP/PS-60/2008).

- ¹ P. G. de Gennes and J. Prost, *The Physics of Liquid Crystals*, 2nd ed. (Oxford Science Publications, Oxford, 1993).
- ² B. Senyuk, J. S. Evans, P. J. Ackerman, T. Lee, P. Manna, L. Vigderman, E. R. Zubarev, J. V. de Lagemaat, and I. I. Smalyukh, *Nano Lett.* **12**, 955 (2012).
- ³ M. B. Pandey, T. Porenta, J. Brewer, A. Burkart, S. Copar, S. Zumer, and I. I. Smalyukh, *Phys. Rev. E* **89**, 060502(R) (2014).
- ⁴ S. Chandrasekhar, *Liquid Crystals*, 2nd ed. (Cambridge University Press, Cambridge, 1994).
- ⁵ H. Stark, *Phys. Rep.* **351**, 387 (2001).
- ⁶ I. Musevic and M. Skarabot, *Soft Matter* **4**, 195 (2008).
- ⁷ G. B. Hadjichristov, Y. G. Marinov, A. G. Petrov, E. Bruno, L. Marino, and N. Scaramuzza, *J. Appl. Phys.* **115**, 083107 (2014).
- ⁸ R. Basu, *Appl. Phys. Lett.* **103**, 241906 (2013).
- ⁹ M. Javad, U. Martin, Y. Kui, S. Heinz, and T. H. Kitzerow, *J. Mater. Chem.* **21**, 12710 (2011).
- ¹⁰ T. Joshi, S. Singh, A. Choudhary, R. P. Pant, and A. M. Biradar, *Appl. Phys. Lett.* **103**, 034110 (2013).
- ¹¹ M. Tasinkevych, F. Mondiot, O. M. Monvalc, and J. C. Loudet, *Soft Matter* **10**, 2047 (2014).
- ¹² U. B. Singh, R. Dhar, R. Dabrowski, and M. B. Pandey, *Liq. Cryst.* **40**, 774 (2013).
- ¹³ Y. Reznikov, O. Buchnev, O. Tereshchenko, V. Reshetnyak, A. Glushchenko, and J. West, *Appl. Phys. Lett.* **82**, 1917 (2003).

- ¹⁴ Y. Tao and Y. H. Tam, *Appl. Phys. Lett.* **103**, 203102 (2013).
- ¹⁵ B. Senyuk, N. Behabtu, B. G. Pacheco, T. Lee, G. Ceriotti, J. M. Tour, M. Pasquali, and I. Smalyukh, *ACS Nano* **6**(9), 8060 (2012).
- ¹⁶ S. Kumar, S. K. Pal, P. S. Kumar, and V. Lakshminarayanan, *Soft Matter* **3**, 896 (2007).
- ¹⁷ J. K. Whitmer, A. A. Joshi, T. F. Roberts, and J. J. de Pablo, *J. Chem. Phys.* **138**, 194903 (2013).
- ¹⁸ P. C. Huang and W. P. Shih, *Appl. Phys. Lett.* **102**, 243510 (2013).
- ¹⁹ R. Manda, V. Dasari, P. Sathyanarayana, M. V. Rasna, P. Paik, and S. Dhara, *Appl. Phys. Lett.* **103**, 141910 (2013).
- ²⁰ H. Y. Jung, H. J. Kim, S. Yang, Y. G. Kang, B. Y. Oh, H. G. Park, and D. S. Seo, *Liq. Cryst.* **39**, 789 (2012).
- ²¹ A. Lorenz, N. Zimmermann, S. Kumar, D. R. Evans, G. Cook, M. F. Martínez, and H. S. Kitzerow, *J. Phys. Chem. B* **117**, 937 (2013).
- ²² S. K. Prasad, M. V. Kumar, T. Shilpa, and C. V. Yelamaggad, *RSC Adv.* **4**, 4453 (2014).
- ²³ T. Stieger, M. Schoen, and M. G. Mazza, *J. Chem. Phys.* **140**, 054905 (2014).
- ²⁴ D. Bera, L. Qian, and P. H. Holloway, *Phosphor Quantum Dots*; John Wiley & Sons, Ltd, West Sussex, UK, 2008.
- ²⁵ S. A. McDonald, G. Konstantatos, S. Zhang, P. W. Cyr, E. J. D. Klem, L. Levina, and E. H. Sargent, *Nat. Mater.* **4**, 138 (2005).
- ²⁶ A. V. Baranov, A. O. Orlova, V. G. Maslov, Y. A. Toporova, E. V. Ushakova, A. V. Fedorov, S. A. Cherevko, M. V. Artemyev, T. S. Perova, and K. Berwick, *J. Appl. Phys.* **108**, 074306 (2010).
- ²⁷ S. Kumar and L. K. Sagar, *Chem. Commun.* **47**, 12182 (2011).
- ²⁸ S. Mohyeddine, M. B. Pandey, and D. Revannasiddaiah, *Phase Transitions* **82**, 11 (2009).